

UC Santa Barbara

UC Santa Barbara Previously Published Works

Title

Oxo Ligand Substitution in a Cationic Uranyl Complex: Synergistic Interaction of an Electrophile and a Reductant

Permalink

<https://escholarship.org/uc/item/8ff3t87n>

Journal

Inorganic Chemistry, 54(14)

ISSN

0020-1669

Authors

Pedrick, Elizabeth A
Wu, Guang
Hayton, Trevor W

Publication Date

2015-07-20

DOI

10.1021/acs.inorgchem.5b01077

Peer reviewed

**Oxo Ligand Substitution in a Cationic Uranyl Complex: Synergistic
Interaction of an Electrophile and a Reductant**

Elizabeth A. Pedrick, Guang Wu, and Trevor W. Hayton*

Department of Chemistry and Biochemistry, University of California Santa

Barbara, Santa Barbara, CA 93106

*To whom correspondence should be addressed. Email: hayton@chem.ucsb.edu

Abstract

Reaction of $[\text{U}^{\text{VI}}\text{O}_2(\text{dppmo})_2(\text{OTf})][\text{OTf}]$ ($\text{dppmo} = \text{Ph}_2\text{P}(\text{O})\text{CH}_2\text{P}(\text{O})\text{Ph}_2$) with 4 equiv of Ph_3SiOTf and 2 equiv of Cp_2Co , generates the U(IV) complex, $\text{U}^{\text{IV}}(\text{OTf})_4(\text{dppmo})_2$ (**1**), as a yellow-green crystalline solid in 83% yield, along with $\text{Ph}_3\text{SiOSiPh}_3$ and $[\text{Cp}_2\text{Co}][\text{OTf}]$. This reaction proceeds via a U(IV) silyloxy intermediate, $[\text{U}^{\text{IV}}(\text{OSiPh}_3)(\text{dppmo})_2(\text{OTf})_2][\text{OTf}]$ (**2**), which we have isolated and structurally characterized. Similarly, reaction of $[\text{U}^{\text{VI}}\text{O}_2(\text{TPPO})_4][\text{OTf}]_2$ ($\text{TPPO} = \text{Ph}_3\text{PO}$) with 6 equiv of Me_3SiOTf and 2 equiv Cp_2Co , generates the U(IV) complex, $[\text{Cp}_2\text{Co}][\text{U}^{\text{IV}}(\text{OTf})_5(\text{TPPO})_2]$ (**3**), as a yellow-green crystalline solid in 76% yield, concomitant with formation of $\text{Me}_3\text{SiOSiMe}_3$, $[\text{Ph}_3\text{POSiMe}_3][\text{OTf}]$, and $[\text{Cp}_2\text{Co}][\text{OTf}]$. Complexes **1** and **3** have been fully characterized, including analysis by X-ray crystallography. The conversion of $[\text{U}^{\text{VI}}\text{O}_2(\text{dppmo})_2(\text{OTf})][\text{OTf}]$ and $[\text{U}^{\text{VI}}\text{O}_2(\text{TPPO})_4][\text{OTf}]_2$ to complexes **1** and **3**, respectively, represent rare examples of well-defined uranyl oxo ligand substitution in a cationic uranyl complex.

Introduction

Reductive silylation of the uranyl ion was first reported in 2008,¹ and has since been described for a variety of co-ligand types and silylating reagents.²⁻⁷ For example, Arnold and co-workers demonstrated that sequential reaction of $U^{VI}O_2(THF)(H_2L)$ (L = polypyrrolic macrocycle) with $KN(SiMe_3)_2$ and FeI_2 resulted in formation of the U(V) silyloxide, $[U^V(O)(OSiMe_3)(THF)Fe_2I_2L]$.⁷ Similarly, our research group has demonstrated that reaction of $U^{VI}O_2(Aracnac)_2$ ($Aracnac = ArNC(Ph)CHC(Ph)O$, $Ar = 3,5-tBu_2C_6H_3$),⁸ with a mixture of $B(C_6F_5)_3$ and $HSiR_3$ ($R = Ph, Et$),^{9,10} or with Ph_3SiOTf alone,¹¹ results in formation of the reductive silylation products, $U^V(OSiR_3)(OB\{C_6F_5\}_3)(Aracnac)_2$,^{9,10} and $[U^V(OSiPh_3)_2(Aracnac)_2][OTf]$,¹¹ respectively. In contrast to these oxo functionalization reactions, examples of complete oxo substitution remain rare. For instance, Ephritikhine and co-workers reported that reaction of $U^{VI}O_2I_2$ with Me_3SiX ($X = Cl, Br, I$) in MeCN resulted in formation of $U^{IV}X_4(MeCN)_4$.¹² In this example, the uranyl oxo ligand is likely converted into $Me_3SiOSiMe_3$.¹³ Thionyl chloride can also effect oxo ligand substitution, as observed upon conversion of $[U^{VI}O_2Cl_4]^{2-}$ to $[U^{VI}OCl_5]^-$.¹⁴ In addition, our research group recently demonstrated a two-step procedure for the controlled removal of a uranyl oxo ligand, wherein a uranyl oxo was converted into a silyloxide that was subsequently protonated with a weak acid.¹⁵

It is notable that many reductive silylation reactions can only achieve a 1e⁻ reduction of the metal center.^{1,2,9,10} Achieving a 2e⁻ reduction, which would allow for isolation of a U(IV) product, appears to be more difficult, and only a few examples are known, including the Ephritikhine example discussed in the preceding paragraph.¹² Other examples include the reaction of $U^{VI}O_2(t^Buacnac)_2$ ($t^Buacnac = t^BuNC(Ph)CHC(Ph)O$) with Me_3SiI/Ph_3P , followed by addition of 2,2'-bipyridine (bipy),¹⁶ and the stepwise reaction of $U^{VI}O_2(Aracnac)_2$ with $B(C_6F_5)_3/HSiPh_3$ and Cp_2Co .⁹ Both transformations result in the

formation of U(IV) bis(silyloxy) complexes as the final products; however, both transformations are two step processes that require the isolation of an intermediate. This paucity of examples can be rationalized on the basis of the strongly electron donating ligands, such as ^{Ar}acnac or the pacman macrocycle,¹ which are often used in this chemistry, as these tend to stabilize higher oxidation states. As a result, the products of these reactions often have U(V)/U(IV) redox potentials that are a challenge to access chemically. For example, the U(V) reductive silylation product, U^V(OSiPh₃)(OB{C₆F₅}₃)(^{Ar}acnac)₂, features a rather low U(V)/U(IV) redox potential of -0.72 V (vs. Fc/Fc⁺).⁹ These strongly-donating ligands are nonetheless beneficial because they weaken the axial ligand field, thereby rendering the oxo ligands more nucleophilic and making the initial silylation step easier.

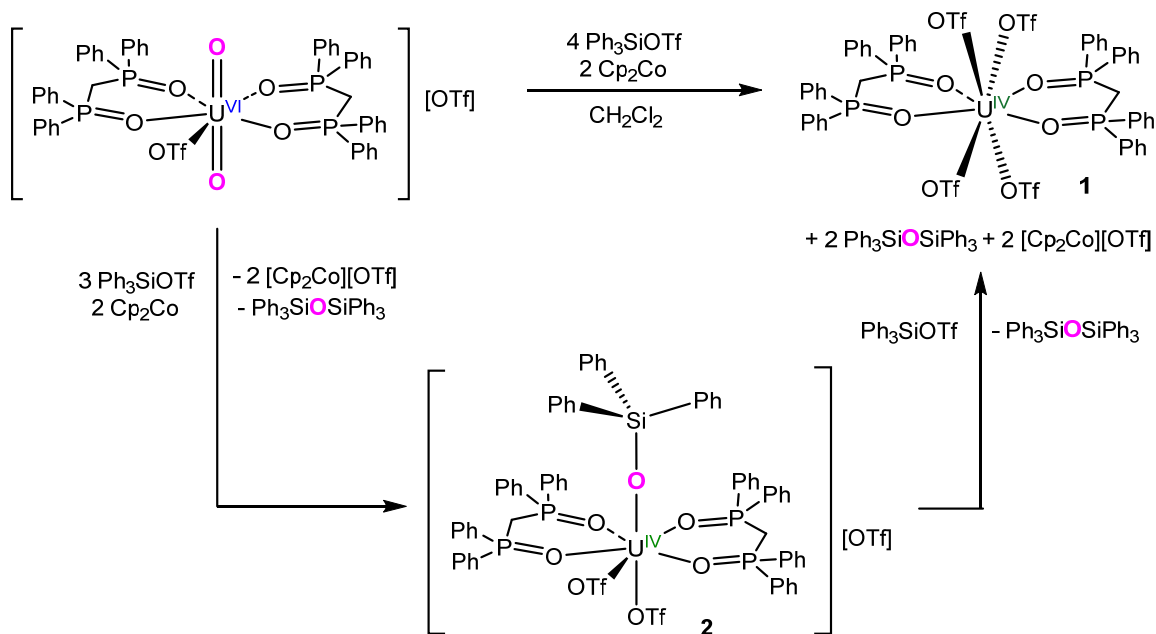
Herein, we describe our attempts to perform reductive silylation on [U^{VI}O₂(dppmo)₂(OTf)][OTf] (dppmo = Ph₂P(O)CH₂P(O)Ph₂) and [U^{VI}O₂(TPPO)₄][OTf]₂ (TPPO = Ph₃PO). These complexes were chosen, in part, because their cationic charges should make reduction to U(IV) more facile, potentially enabling a 2e⁻ reductive silylation reaction. These favorable redox properties are evidenced indirectly by their U=O(sym) vibrational modes, as it has been previously demonstrated that less negative uranyl 1e⁻ reduction potentials correlate with higher energy U=O(sym) stretches.¹⁷ In particular, [U^{VI}O₂(dppmo)₂(OTf)][OTf] and [U^{VI}O₂(TPPO)₄][OTf]₂ feature U=O(sym) stretches of 849 cm⁻¹,¹⁸ and 839 cm⁻¹, respectively, which are notably higher in energy than those exhibited by U^{VI}O₂(^{Ar}acnac)₂ (812 cm⁻¹),¹⁶ or U^{VI}O₂(dbm)₂(THF) (dbm = OC(Ph)CHC(Ph)O) (823 cm⁻¹).¹⁵ However, their higher energy uranyl U=O(sym) stretches also suggests that their oxo ligands will be less nucleophilic, which will disfavor oxo ligand silylation.

Results and Discussion

Previously, we demonstrated that reaction of the U^{VI}O₂(dbm)₂(THF) with 2 equiv Ph₃SiOTf resulted in silylation of both oxo ligands and 1e⁻ reduction of the uranium center.¹¹

In contrast, exposure of $[\text{U}^{\text{VI}}\text{O}_2(\text{dppmo})_2(\text{OTf})][\text{OTf}]$ to the same protocol¹¹ resulted in no reaction, according to ^1H and $^{19}\text{F}\{^1\text{H}\}$ NMR spectroscopies (Figure S13-S15). This was somewhat surprising considering that Ph_3SiOTf was developed specifically as a reductive silylation reagent,¹¹ but it is nonetheless consistent with our hypothesis that the oxo ligands in $[\text{U}^{\text{VI}}\text{O}_2(\text{dppmo})_2(\text{OTf})][\text{OTf}]$ are less nucleophilic than those in $\text{U}^{\text{VI}}\text{O}_2(\text{dbm})_2(\text{THF})$ or $\text{U}^{\text{VI}}\text{O}_2(\text{Aracnac})_2$.¹⁵ Gratifyingly, though, reaction of $[\text{U}^{\text{VI}}\text{O}_2(\text{dppmo})_2(\text{OTf})][\text{OTf}]$ with 4 equiv of Ph_3SiOTf , in the presence of 2 equiv of Cp_2Co , results in a rapid reaction, as evidenced by a color change from pale yellow to dark yellow-green. Work-up of the reaction mixture after 24 h results in the isolation of the U(IV) triflate complex, $\text{U}^{\text{IV}}(\text{OTf})_4(\text{dppmo})_2$ (**1**), as a lime green powder in an 83% yield (Scheme 1). Complex **1** is the result of complete oxo ligand removal from the uranyl ion, concomitant with a $2e^-$ reduction.

Scheme 1.



Complex **1** co-crystallizes with 1 equiv of cobaltocenium triflate in the lattice as a toluene and hexane solvate, $[\mathbf{1}][\text{Cp}_2\text{Co}][\text{OTf}] \cdot 1.5\text{C}_7\text{H}_8 \cdot \text{C}_6\text{H}_{14}$. Its solid-state molecular

structure is shown in Figure 1 and selected bond lengths and angles are collected in Table 1. Complex **1** features a square antiprism geometry, according to the continuous shape measure developed by Alvarez and co-workers (CSM = 0.32),¹⁹ wherein the two square faces are defined by O1, O4, O7, and O8, and O2, O3, O5, and O6, respectively. The average U-O_{OTf} distance (av. U-O = 2.39 Å) is similar to other U(IV)-O_{OTf} distances,²⁰⁻²² but is slightly longer than those observed in the structurally related complex, U^{IV}(OTf)₄(DME)₂ (av. U-O = 2.28 Å),²³ which is probably a result of the steric bulk of the dppmo ligands. In addition, the average U-O_{dppmo} bond length (av. U-O = 2.31 Å) is slightly shorter than the average U-O_{dppmo} distance in the uranyl starting material, [U^{VI}O₂(dppmo)₂(OTf)][OTf] (av. U-O = 2.38 Å),¹⁸ but is similar to other U(IV) phosphine oxide complexes.²⁴⁻²⁶

Table 1. Selected Bond Lengths (Å) and Angles (deg) for Complexes 1 - 3

	1	2	3
U-O _{Si}		2.073(6)	
U-O _{OTf} (η ²)		2.614(9) 2.622(8)	
U-O _{OTf} (η ¹)	2.36(1) 2.36(1) 2.40(1) 2.44(1)	2.391(7)	2.308(5) 2.312(4) 2.337(4) 2.340(4) 2.341(4)
U-O _{dppmo/TPPO}	2.27(2) 2.28(1) 2.30(2) 2.38(1)	2.341(6) 2.346(6) 2.354(6) 2.359(6)	2.186(4) 2.197(4)
O-Si		1.647(7)	
O _{Si} -U-O _{OTf}		163.2(3)	
U-O-Si		166.6(4)	

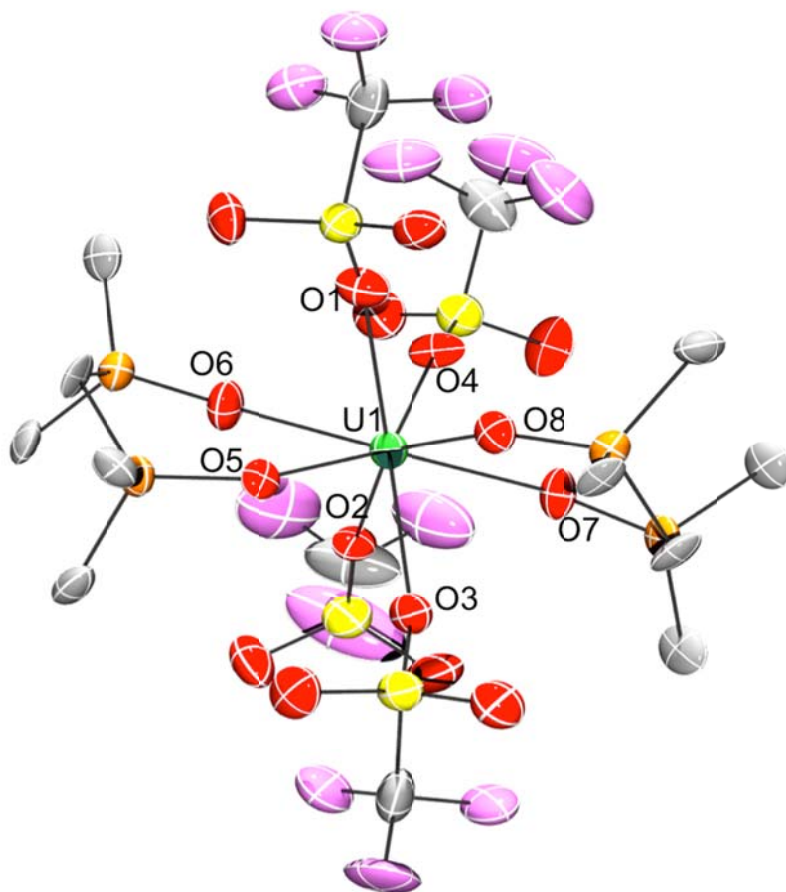


Figure 1. Solid-state structure of $[U^{IV}(OTf)_4(dppmo)_2] \cdot [Cp_2Co][OTf] \cdot 1.5C_7H_8 \cdot C_6H_{14}$ ($[1][Cp_2Co][OTf] \cdot 1.5C_7H_8 \cdot C_6H_{14}$) with 50% probability ellipsoids. All hydrogens, the phenyl rings on the dppmo backbone, the co-crystallized cobaltocenium triflate, toluene and hexane solvates have been removed for clarity.

The 1H NMR spectrum of complex **1** in CD_2Cl_2 exhibits a broad resonance at 32.75 ppm, corresponding to the γ -proton environment on the dppmo ligands (Figure S2). In addition, this spectrum features singlets at 15.25, 8.89, and 8.67 ppm, which correspond to the *o*-, *p*-, and *m*- resonances of the phenyl rings on the dppmo backbone, respectively. Finally, a singlet at 5.70 ppm is assignable to the co-crystallized $[Cp_2Co]^+$ moiety. The $^{19}F\{^1H\}$ NMR spectrum of **1** exhibits two extremely broad resonances at -97.26 and -77.18

ppm, which can be attributed to the OTf environment in complex **1** and the OTf anion in $[\text{Cp}_2\text{Co}][\text{OTf}]$,²⁷ respectively (Figure S3). The broadness of these resonances is suggestive of exchange of the inner- and outer-sphere triflate moieties at a rate that is comparable to the NMR time scale. The $^{31}\text{P}\{^1\text{H}\}$ NMR spectrum of **1** does not feature any resonances, possibly because they are too broad to be observed. In addition, the near-IR spectrum for **1** is similar to those of other U(IV) complexes (Figure S30),^{9,10,28,29} supporting the presence of a $5f^2$ ion.

To better understand the mechanism of formation of complex **1**, and determine the fate of the “yl” oxygen atoms, we followed the reaction of $[\text{U}^{\text{VI}}\text{O}_2(\text{dppmo})_2(\text{OTf})][\text{OTf}]$ with 4 equiv of Ph_3SiOTf and 2 equiv of Cp_2Co , in CD_2Cl_2 , by ^1H and $^{19}\text{F}\{^1\text{H}\}$ NMR spectroscopies. The ^1H NMR spectrum after 20 min reveals the formation of $[\text{Cp}_2\text{Co}]^+$, as evidenced by a resonance at 5.35 ppm (Figure S4).²⁷ Complex **1** is not present in the reaction mixture at these short reaction times; however, several new uranium-containing complexes are observed in the reaction mixture. These intermediates are evidenced by the appearance of downfield resonances at 47.85, 41.70 and 36.91 ppm, which are assignable to the *ortho*-CH proton environments of the $[\text{OSiPh}_3]^-$ ligand for three different uranium-containing intermediates. We have tentatively assigned the resonance at 47.85 ppm to a U(IV) bis(silyloxy) complex. In addition, we have assigned the resonance at 36.91 ppm to a U(IV) mono(silyloxy) complex, $[\text{U}^{\text{IV}}(\text{OSiPh}_3)(\text{dppmo})_2(\text{OTf})_2][\text{OTf}]$ (**2**) (see below). These two species are likely intermediates formed along the reaction pathway to **1**. Consistent with this hypothesis, the ^1H NMR spectrum of the reaction mixture after 2 h reveals the complete disappearance of the resonance at 47.85 ppm, the continued presence of **2**, and the appearance of complex **1**, as evidenced by the observation of a broad resonance at 33.41 ppm, which is assignable to the γ - CH_2 environment of the dppmo ligand. After 24 h, the ^1H NMR spectrum of the reaction mixture reveals the complete disappearance of complex **2**, along with the expected presence of complex **1**. Interestingly, complex **1** is not very soluble

under these conditions and it partially precipitates from solution. The *in situ* $^{19}\text{F}\{^1\text{H}\}$ NMR spectra are consistent with this reaction sequence. For example, the *in situ* $^{19}\text{F}\{^1\text{H}\}$ NMR spectrum after 20 min reveals the presence of outer sphere $[\text{OTf}]^-$, along with a resonance at -114.19 ppm, which we have tentatively assigned to the OTf environment of a U(IV) bis(silyloxy) intermediate. After 2 h, this resonance disappears, concomitant with the appearance of a new resonance 97.24 ppm, which is assignable to complex **1** (Figure S6). Finally, a $^{29}\text{Si}\{^1\text{H}\}$ NMR spectrum of the reaction mixture, in TCE- d_2 (TCE = 1,1,2,2-tetrachloroethane), consists of a singlet at -17.83 ppm, which is assignable to $\text{Ph}_3\text{SiOSiPh}_3$ ³⁰ (Figure S7), confirming the final fate of uranyl oxo ligands.

Interestingly, addition of 2 equiv of Cp_2Co to a solution of $[\text{U}^{\text{VI}}\text{O}_2(\text{dppmo})_2(\text{OTf})][\text{OTf}]$ results in the consumption of the uranyl starting material and the formation of free dppmo and $[\text{Cp}_2\text{Co}][\text{OTf}]$ (Figures S9-S12); however, we have been unable to identify the uranium-containing products of this reaction. Moreover, addition of 1 equiv of Cp_2Co to Ph_3SiOTf in CD_2Cl_2 results in no reaction over the course of 30 min (Figure S8). When combined with the knowledge that $[\text{U}^{\text{VI}}\text{O}_2(\text{dppmo})_2(\text{OTf})][\text{OTf}]$ does not react with Ph_3SiOTf , these experiments reveal the synergistic relationship between Cp_2Co and Ph_3SiOTf that is required to form **1**. To explain these observations, and rationalize the observed *in situ* NMR spectra, we postulate that **1** is formed via a series of intermediate steps (Scheme S1). First, Cp_2Co reduces $[\text{U}^{\text{VI}}\text{O}_2(\text{dppmo})_2(\text{OTf})][\text{OTf}]$, transiently forming $\text{U}^{\text{V}}\text{O}_2(\text{dppmo})_2(\text{OTf})$, which is then captured by 2 equiv of Ph_3SiOTf to form a U(V) bis(silyloxy) intermediate. In the absence of Ph_3SiOTf , $\text{U}^{\text{V}}\text{O}_2(\text{dppmo})_2(\text{OTf})$ likely decomposes, as evidenced by the formation of free dppmo in the reaction of $[\text{U}^{\text{VI}}\text{O}_2(\text{dppmo})_2(\text{OTf})][\text{OTf}]$ with 2 equiv of Cp_2Co (Figure S10). The U(V) bis(silyloxy) intermediate subsequently reacts with a further equivalent of Cp_2Co to generate the U(IV) bis(silyloxy) intermediate and $[\text{Cp}_2\text{Co}][\text{OTf}]$. The U(IV) bis(silyloxy) intermediate then

reacts with a third equiv of Ph₃SiOTf, to generate complex **2** and 1 equiv of Ph₃SiOSiPh₃, whereupon complex **2** reacts with the final equiv of Ph₃SiOTf, to afford complex **1** and the second equiv of Ph₃SiOSiPh₃. Most importantly, the reduction of [U^{VI}O₂(dppmo)₂(OTf)][OTf] to a neutral U(V) complex should render the uranyl oxo ligands more nucleophilic, which nicely rationalizes why Ph₃SiOTf is an ineffective silylating reagent in the absence of Cp₂Co.

In an attempt to isolate the hypothesized U(IV) silyloxy intermediates, and buttress the proposed mechanism, the reaction of [U^{VI}O₂(dppmo)₂(OTf)][OTf] with 4 equiv of Ph₃SiOTf and 2 equiv of Cp₂Co was left to stand, unstirred, at room temperature for 15 h. Work-up of this reaction mixture results in isolation of a crystalline mixture that contained the U(IV) monosilyloxy complex, [U^{IV}(OSiPh₃)(dppmo)₂(OTf)₂][OTf] (**2**), and [Cp₂Co][OTf] (Scheme 1). The identity of both materials was confirmed by X-ray crystallography. Notably, complex **1** was not formed in this reaction, according to a ¹H NMR spectrum of the reaction mixture, which may be a function of the lack of stirring and shorter reaction time.

Complex **2** crystallizes in the monoclinic space group *P2₁/n* as a dichloromethane and diethyl ether solvate, **2**·3CH₂Cl₂·C₄H₁₀O (Figure 2). Selected bond lengths and angles can be found in Table 1. In the solid state, complex **2** features two dppmo ligands, a [OSiPh₃]⁻ ligand, an η¹-OTf ligand, and an η²-OTf ligand, in a bi-capped trigonal prismatic geometry (CSM = 1.91).¹⁹ The U-O_{Si} distance is 2.073(6) Å, which is comparable to other U(IV) silyloxy distances,⁹ including those of U^{IV}(OSiMe₃)₂I₂(bipy)₂ (2.084(4) Å),¹⁶ U^{IV}(OSiEt₃)₂(^{Ar}acnac)₂ (2.129(2) Å),¹⁰ and Cp₃U^{IV}(OSiPh₃) (2.135(8) Å).³¹ The U-O distance of the η¹-bound OTf moiety (2.391(7) Å) is similar to that of the uranyl starting material, [U^{VI}O₂(dppmo)₂(OTf)][OTf] (2.408(3) Å),¹⁸ while the U-O distances of the η²-bound OTf ligand (2.614(9) and 2.622(8) Å) are substantially longer. Finally, the average U-O_{dppmo} bond length (av. U-O = 2.35 Å) is similar to that of the uranyl starting material (av. U-O = 2.38 Å).¹⁸

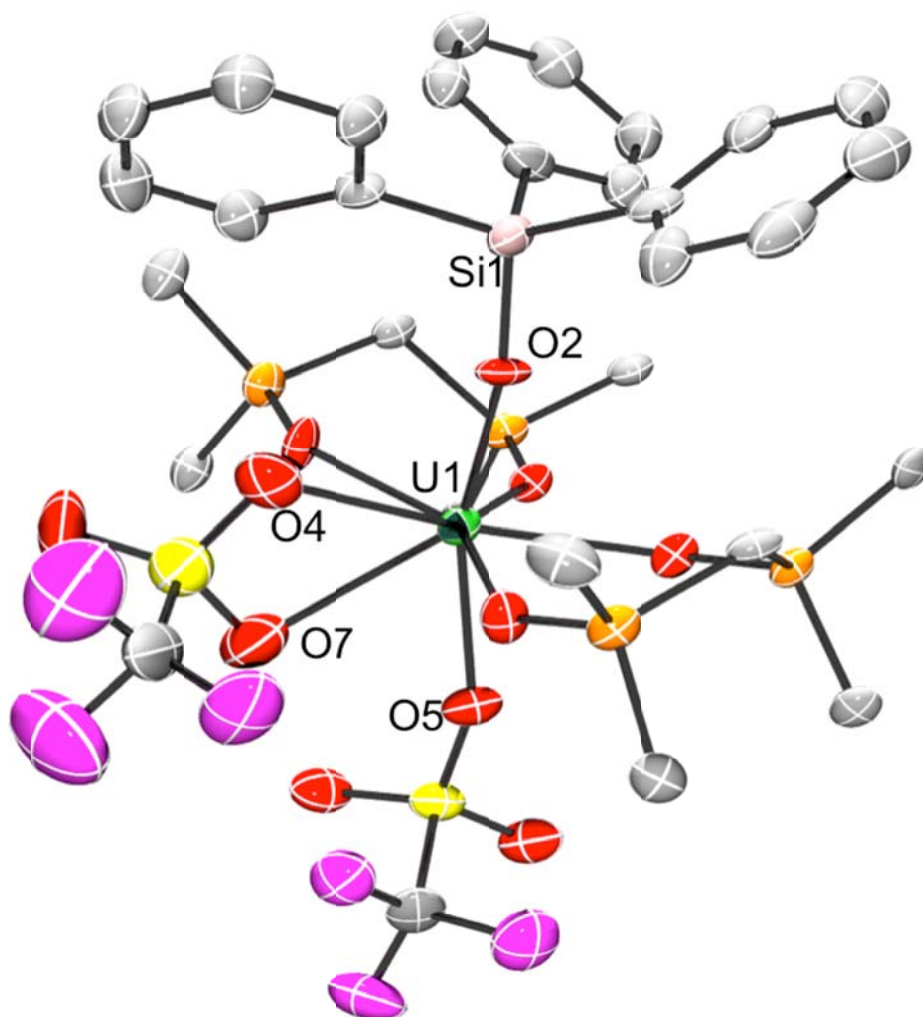
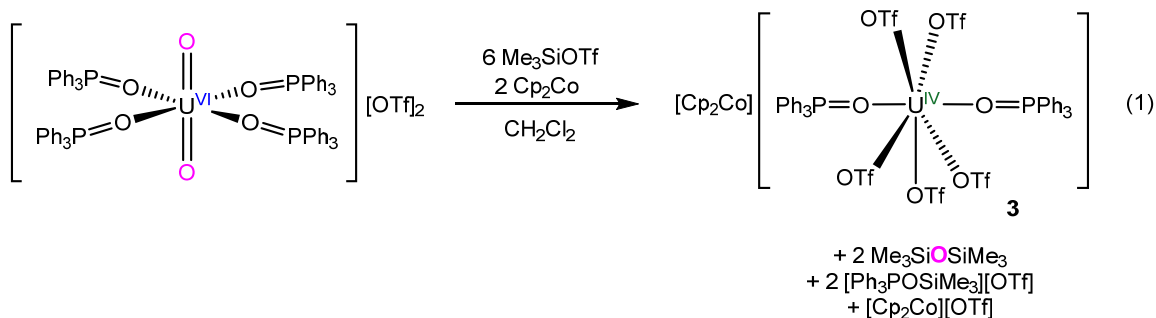


Figure 2. Solid-state structure of $[U^{IV}(OSiPh_3)(dppmo)_2(OTf)_2][OTf] \cdot 3CH_2Cl_2 \cdot C_4H_{10}O$ ($2 \cdot 3CH_2Cl_2 \cdot C_4H_{10}O$) with 50% probability ellipsoids. All hydrogens, the phenyl rings on the dppmo backbone, the OTf counter ion, and the CH_2Cl_2 and diethyl ether solvates have been removed for clarity.

The 1H NMR spectrum of the isolated mixture of **2** and $[Cp_2Co][OTf]$ in CD_2Cl_2 features three narrow resonances at 37.86, 12.57, and 11.72 ppm, which correspond to the *o*-, *m*-, and *p*-proton environments of the $[Ph_3SiO]^-$ ligand, respectively (Figure S16). Importantly, these resonances are nearly identical to those observed during the *in situ*

monitoring of the formation of complex **1** (see text above and Figure S4), confirming its identity as one of the intermediates in the reaction. The ^1H NMR spectrum also features a resonance at 5.73 ppm, which is assignable to the $[\text{Cp}_2\text{Co}]^+$ ion.²⁷ The $^{19}\text{F}\{^1\text{H}\}$ NMR spectrum of this mixture features a single resonance at -80.36 ppm, which corresponds to the $[\text{OTf}]^-$ environment in $[\text{Cp}_2\text{Co}][\text{OTf}]$ (Figure S17). No ^{19}F resonance was observed that could be reasonably assigned to complex **2**, possibly because of rapid exchange between its inner sphere and outer sphere $[\text{OTf}]^-$ moieties. Likewise, the $^{31}\text{P}\{^1\text{H}\}$ NMR spectrum of this mixture featured no observed resonances. Due to our inability to separate **2** from $[\text{Cp}_2\text{Co}][\text{OTf}]$, complete characterization of complex **2** could not be completed. Nonetheless, we were able to perform some reactivity studies with this material. For example, reaction of **2**, contaminated with a small amount of $[\text{Cp}_2\text{Co}][\text{OTf}]$, with 1 equiv Ph_3SiOTf in CD_2Cl_2 was monitored by ^1H NMR spectroscopy (Figures S18-S19). As anticipated, this experiment revealed the formation of small amounts of complex **1** after 5 h, consistent with the reaction pathway presented in Scheme 1.



To further our insight into the reductive silylation of cationic uranyl complexes, we attempted the reductive silylation of $[\text{U}^{\text{VI}}\text{O}_2(\text{TPPO})_4][\text{OTf}]_2$. This complex features a comparable $\text{U}=\text{O}$ ν_{sym} value to that of $[\text{U}^{\text{VI}}\text{O}_2(\text{dppmo})_2(\text{OTf})][\text{OTf}]$, suggesting that it is a similarly difficult substrate for the reductive silylation reaction. Thus, addition of 6 equiv of Me_3SiOTf and 2 equiv of Cp_2Co to a cold CH_2Cl_2 solution of $[\text{U}^{\text{VI}}\text{O}_2(\text{TPPO})_4][\text{OTf}]_2$ results in

formation of $[\text{Cp}_2\text{Co}][\text{U}^{\text{IV}}(\text{OTf})_5(\text{TPPO})_2]$ (**3**), which can be isolated as a yellow-green crystalline material in a 76% yield (eq 1). Also formed in this reaction are $\text{Me}_3\text{SiOSiMe}_3$ ³² and $[\text{Ph}_3\text{POSiMe}_3][\text{OTf}]$ ³³⁻³⁵ (eq 1), according to the $^{29}\text{Si}\{^1\text{H}\}$ and $^{31}\text{P}\{^1\text{H}\}$ NMR spectra of the reaction mixture (Figures S23-S24). Moreover, the reagents must be cooled to $-25\text{ }^\circ\text{C}$ before the reaction, otherwise significant amounts of intractable black precipitate (possibly UO_2) are formed instead. Complex **3** can also be formed by addition of 6 equiv of Ph_3SiOTf , and 2 equiv of Cp_2Co , to $[\text{U}^{\text{VI}}\text{O}_2(\text{TPPO})_4][\text{OTf}]_2$; however, the by-products formed in this case proved difficult to separate from complex **3**. Importantly, reaction of $[\text{U}^{\text{VI}}\text{O}_2(\text{TPPO})_4][\text{OTf}]_2$ with only Me_3SiOTf results in formation of $[\text{Ph}_3\text{POSiMe}_3][\text{OTf}]$, but does not result in any oxo ligand silylation (Figure S26). In addition, reaction of $[\text{U}^{\text{VI}}\text{O}_2(\text{TPPO})_4][\text{OTf}]_2$ with only Cp_2Co results in a slow transformation, similar to that observed between $[\text{U}^{\text{VI}}\text{O}_2(\text{dppmo})_2(\text{OTf})][\text{OTf}]$ and Cp_2Co (Figure S25), while no reaction is observed between Me_3SiOTf and Cp_2Co (Figure S27). Overall, these data point to a synergistic relationship between Me_3SiOTf and Cp_2Co during the conversion of uranyl to U(IV), similar to that observed during formation of **1**.

Complex **3** crystallizes in the monoclinic space group $P2_1/c$ as a discrete cation/anion pair. Its solid-state molecular structure is shown in Figure 3 and selected bond lengths and angles are collected in Table 1. The U(IV) center in **3** features a pentagonal bipyramidal (CSM = 1.74) geometry,¹⁹ wherein two TPPO ligands occupy the axial positions and the five η^1 -OTf ligands occupy the equatorial plane. The average U- O_{OTf} distance (av. U-O = 2.33 Å) is typical of those in other U(IV)-triflate complexes,²⁰⁻²² but is slightly shorter than those seen in complex **1**, which we attribute to the reduced steric bulk of TPPO vs. dppmo. In addition, the two U- O_{TPPO} bond lengths (2.186(4) and 2.197(4) Å) are both shorter than the U- O_{dppmo} distance observed for **1**, which is also consistent with the reduced steric profile of TPPO vs. dppmo.

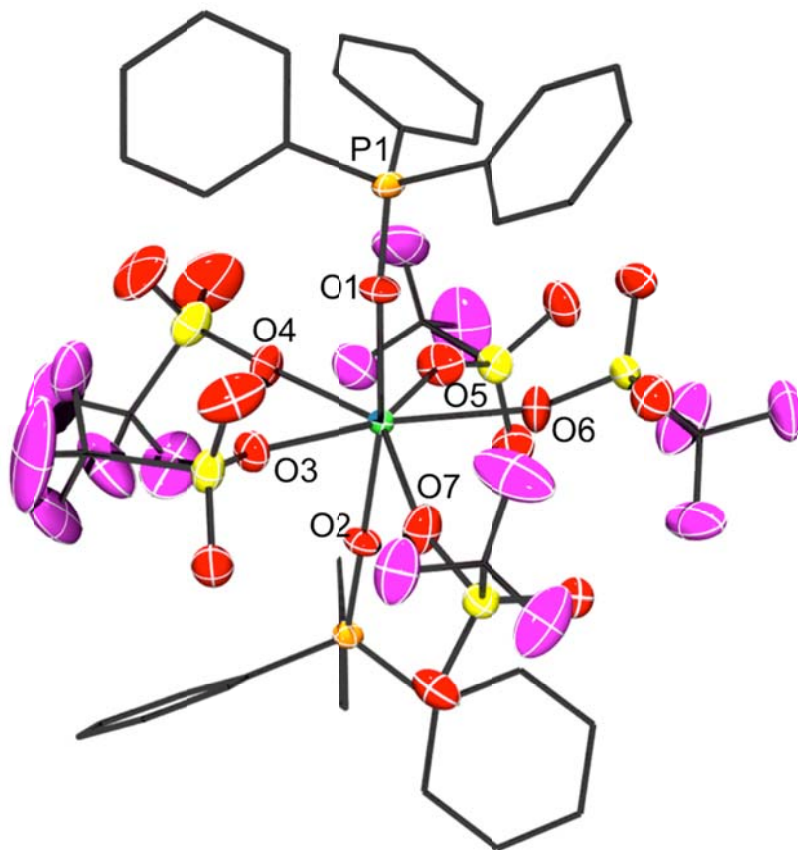


Figure 3. Solid-state molecular structure of $[\text{Cp}_2\text{Co}][\text{U}^{\text{IV}}(\text{OTf})_5(\text{TPPO})_2]$ (**3**) with 50% probability ellipsoids. All hydrogen atoms and the cobaltocenium cation have been removed for clarity.

The ^1H NMR spectrum of **3** at room temperature consists of three broad resonances at 31.66, 12.04, and 11.16 ppm, assignable to the *o*-, *m*-, and *p*- phenyl protons of the TPPO ligand, respectively (Figure S20). In addition, this spectrum also features a sharp resonance at 5.70 ppm, which is assignable to the $[\text{Cp}_2\text{Co}]^+$ counterion.²⁷ Surprisingly, the room temperature $^{19}\text{F}\{^1\text{H}\}$ NMR spectrum of **3** features two very broad resonances at -79.06 and -101.02 ppm (Figure S21). We tentatively, assign the former resonance to an outer sphere OTf anion, while the latter resonance is likely due to a uranium-coordinated OTf ligand. To explain this result, we suggest that complex **3** undergoes partial $[\text{OTf}]^-$ dissociation in

solution, to form a mixture of **3**, $\text{U}^{\text{IV}}(\text{OTf})_4(\text{TPPO})_2$ and $[\text{Cp}_2\text{Co}][\text{OTf}]$. Finally, the near-IR spectrum for **3** is similar to those of other U(IV) complexes (Figure S31),^{9,10,28,29} supporting the presence of an $5f^2$ ion.

Concluding Remarks

In summary, reaction of $[\text{U}^{\text{VI}}\text{O}_2(\text{dppmo})_2(\text{OTf})][\text{OTf}]$ with 4 equiv of Ph_3SiOTf and 2 equiv of Cp_2Co , generates the U(IV) complex, $\text{U}^{\text{IV}}(\text{OTf})_4(\text{dppmo})_2$ (**1**). Also formed in this reaction is $\text{Ph}_3\text{SiOSiPh}_3$, which is the product of oxo ligand silylation. Similarly, reaction of $[\text{U}^{\text{VI}}\text{O}_2(\text{TPPO})_4][\text{OTf}]_2$ with 6 equiv of Me_3SiOTf and 2 equiv Cp_2Co , generates the U(IV) complex, $[\text{Cp}_2\text{Co}][\text{U}^{\text{IV}}(\text{OTf})_5(\text{TPPO})_2]$ (**3**), along with $\text{Me}_3\text{SiOSiMe}_3$. The formation of complexes **1** and **3** represent rare examples of uranyl oxo ligand substitution, as well as novel examples of one-pot reductions of uranyl to U(IV), at ambient temperatures and pressures. Interestingly, neither Ph_3SiOTf nor Me_3SiOTf alone are capable of reductively silylating $[\text{U}^{\text{VI}}\text{O}_2(\text{dppmo})_2(\text{OTf})][\text{OTf}]$ or $[\text{U}^{\text{VI}}\text{O}_2(\text{TPPO})_4][\text{OTf}]_2$. Instead, these reagents required the aid of an external reductant, namely, Cp_2Co . This synergistic relationship between Cp_2Co and R_3SiOTf makes it possible to perform reductive silylation on more challenging uranyl substrates, such as cationic uranyl complexes, further expanding the scope of the reductive silylation reaction.

EXPERIMENTAL SECTION

General. All reactions and subsequent manipulations were performed under anaerobic and anhydrous conditions under an atmosphere of nitrogen. Hexanes, toluene and diethyl ether were dried using a Vacuum Atmospheres DRI-SOLV solvent purification system. CH_2Cl_2 , CD_2Cl_2 , and $\text{TCE-}d_2$ were dried over activated 3 Å molecular sieves for 24 h before use.

$\text{U}^{\text{VI}}\text{O}_2\text{Cl}_2(\text{THF})_2$,³⁶ dppmo ,³⁷ and Ph_3SiOTf ,³⁸ were synthesized according to previously reported procedures. Cp_2Co was purchased from Acros Organics and recrystallized from concentrated diethyl ether before use. All other reagents were purchased from commercial suppliers and used as received.

NMR spectra were recorded on a Varian UNITY INOVA 400 spectrometer or an Agilent Technologies 400-MR DD2 spectrometer. ^1H NMR spectra were referenced to external SiMe_4 using the residual protio solvent peaks as internal standards. The chemical shifts of the $^{19}\text{F}\{^1\text{H}\}$ and $^{31}\text{P}\{^1\text{H}\}$ spectra were referenced indirectly with the ^1H resonance of SiMe_4 at 0 ppm, according to IUPAC standard.^{39,40} $^{29}\text{Si}\{^1\text{H}\}$ NMR spectra were referenced to external SiMe_4 in C_6D_6 . Raman and IR spectra were recorded on a Mattson Genesis FTIR/Raman spectrometer. IR samples were recorded as KBr pellets, while Raman samples were recorded in an NMR tube as neat solids. UV-vis/NIR experiments were performed on a UV-3600 Shimadzu spectrophotometer. Elemental analyses were performed by the Microanalytical Laboratory at UC Berkeley.

X-ray Crystallography. Data for **1-3** were collected on a Bruker 3-axis platform diffractometer equipped with a SMART-1000 CCD detector using a graphite monochromator with a $\text{Mo K}\alpha$ X-ray source ($\alpha = 0.71073 \text{ \AA}$). The crystals were mounted on a glass fiber under Paratone-N oil and all data were collected at 100(2) K using an Oxford nitrogen gas cryostream system. A hemisphere of data was collected using ω scans with 0.3° frame widths. Frame exposures of 30, 10, and 10 seconds were used for complexes **1**, **2**, and **3**, respectively. Data collection and cell parameter determinations were conducted using the SMART program.⁴¹ Integration of the data frames and final cell parameter refinement were performed using SAINT software.⁴² Absorption correction of the data was carried out using the multi-scan method SADABS.⁴³ Subsequent calculations were carried out using

SHELXTL.⁴⁴ Structure determinations were done using direct or Patterson methods and difference Fourier techniques. All hydrogen atom positions were idealized, and rode on the atom of attachment. Hydrogen atoms were not assigned to the disordered carbon atoms. Structure solution, refinement, graphics, and creation of publication materials were performed using SHELXTL.⁴⁴

Complex **1** exhibits positional disorder of one hexane solvate molecule. This positional disorder was addressed by modeling the molecule in two positions, in a 50:50 ratio. The EADP, DFIX, and FLAT commands were used to constrain both positions of the hexane molecule. Complex **1** also features a disordered toluene solvate molecule with half occupancy, which overlaps with one position of the hexane solvate. The EADP, DFIX, and FLAT commands were used to constrain the orientation of the toluene molecule. Disordered carbon atoms were not refined anisotropically. In addition, one of the dppmo phenyl rings exhibited mild positional disorder and was constrained using the EADP, DFIX, and FLAT commands. The OTf carbon atoms, two carbon atoms on the [Cp₂Co]⁺, and a few other dppmo carbon atoms were also constrained with the EADP command. For complex **2**, the diethyl ether solvate molecule exhibited mild positional disorder. The EADP, DFIX and FLAT commands were used to constrain its orientation. Disordered atoms were not refined anisotropically. In addition, a few carbon atoms and one oxygen atom of a dppmo ligand were constrained with the EADP command. Finally, one dppmo C-C bond distance was restrained by the DFIX command in complex **3**. A summary of relevant crystallographic data for **1-3** is presented in Table 2.

[U^{VI}O₂(dppmo)₂(OTf)][OTf]. The preparation described below was modified from the published procedure for [U^{VI}O₂(dppmo)₂(TPPO)][OTf]₂.⁴⁵ To a stirring, yellow dichloromethane (3 mL) slurry of U^{VI}O₂Cl₂(THF)₂ (102.8 mg, 0.212 mmol), was added

dropwise a colorless dichloromethane (3 mL) solution of dppmo (175.7 mg, 0.422 mmol). Solid AgOTf (110.2 mg, 0.429 mmol) was then quickly added to the reaction mixture. The reaction mixture was allowed to stir for 24 h at 25 °C, which resulted in formation of a yellow solution concomitant with the deposition of a white precipitate. This solution was filtered through a Celite column supported on glass wool (0.5 cm × 2 cm), which afforded a clear yellow filtrate and a large white plug. The filtrate was concentrated *in vacuo* and layered with diethyl ether (2 mL). Storage of this solution at -25 °C for 24 h resulted in deposition of a pale yellow powder (218.2 mg, 74% yield). Spectral data collected for this material matched those previously reported for this complex, $[U^{VI}O_2(dppmo)_2(OTf)(OTf)]^{18}$

$[U^{VI}O_2(TPPO)_4][OTf]_2$. This complex was prepared according to a modified literature procedure.⁴⁵ To a stirring, yellow dichloromethane (3 mL) slurry of $U^{VI}O_2Cl_2(THF)_2$ (224.0 mg, 0.462 mmol), was added dropwise a colorless dichloromethane (4 mL) solution of TPPO (512.8 mg, 1.843 mmol). Solid AgOTf (275.6 mg, 1.073 mmol) was then quickly added to the reaction mixture. After 3 h, the resulting cloudy yellow solution was filtered through a Celite column supported on glass wool (0.5 cm × 2 cm), which afforded a clear yellow filtrate and a large tan plug. All the volatiles were removed *in vacuo*, which produced a yellow foam. This material was extracted into dichloromethane (8 mL), and filtered through a Celite column supported on glass wool (0.5 cm × 2 cm), which afforded a clear yellow filtrate and a small pale orange plug. The filtrate was then concentrated *in vacuo* and layered with diethyl ether (5 mL). Storage of this solution at -25 °C for 24 h resulted in deposition of a yellow crystalline solid (570.3 mg, 73% yield). Spectral data of this material matched those previously reported for this complex.⁴⁵ Raman (cm⁻¹): 3064(s), 1587(m), 1572(sh w), 1186(w), 1147(w), 1005(m), 1001(s), 839(m, U=O ν_{sym}), 750(w), 685(w), 615(w), 310(w), 253(m).

U^{VI}(OTf)₄(dppmo)₂ (1). To a stirring, pale yellow dichloromethane (2 mL) solution of [U^{VI}O₂(dppmo)₂(OTf)](OTf) (40.4 mg, 0.029 mmol), was added dropwise a dichloromethane (1.5 mL) solution of Ph₃SiOTf (47.2 mg, 0.116 mmol) and Cp₂Co (10.6 mg, 0.058 mmol). This resulted in an immediate color change to green. This solution was allowed to stir for 24 h at 25 °C, which resulted in the deposition of a green precipitate. The mixture was concentrated *in vacuo* and stored at -25 °C for 24 h, which resulted in the further deposition of solid. Isolation of the green powder, followed by dissolution in dichloromethane (4 mL), resulted in formation of a cloudy green solution. This solution was filtered through a Celite column supported on glass wool (0.5 cm × 2 cm), concentrated *in vacuo*, and layered with hexanes (2 mL). Storage of this solution at -25 °C for 24 h, resulted in the deposition of a green crystalline solid, which was isolated by decanting off the supernatant (48.3 mg, 83% yield). X-ray quality crystals of **1**, as a 1:1 co-crystal with [Cp₂Co](OTf), were grown out of a toluene solution layered with hexanes. Anal. Calcd for UO₁₉P₄S₅F₁₅CoC₆₅H₅₂: C, 38.97; H, 2.62. Found: C, 39.36; H, 2.58. ¹H NMR (CD₂Cl₂, 25 °C, 400 MHz): δ 32.75 (br s, 4H, γ-CH), 15.25 (br s, 16H, ortho CH), 8.89 (s, 8H, para CH), 8.67 (s, 16H, meta CH), 5.70 (s, 10H, [Cp₂Co]⁺). ¹⁹F{¹H} NMR (CD₂Cl₂, 25 °C, 376 MHz): δ -77.90 (br s, outer sphere [OTf]⁻), -97.14 (br s, inner sphere [OTf]⁻). UV-vis/NIR (CH₂Cl₂, 4.44 × 10⁻³ M, L·mol⁻¹·cm⁻¹): 398 (ε = 332), 542 (ε = 20), 620 (ε = 30), 636 (ε = 31), 658 (ε = 43), 774 (ε = 9), 828 (ε = 11), 1008 (sh, ε = 14), 1062 (sh, ε = 25), 1112 (ε = 53), 1408 (ε = 16), 1522 (ε = 14), 1636 (ε = 9), 2024 (ε = 3). IR (KBr pellet, cm⁻¹): 1591(w), 1487(w), 1441(m), 1417(w), 1331(m), 1277(s), 1255(s), 1234(s), 1221(s sh), 1203(vs), 1163(s sh), 1126(vs), 1074(s sh), 1068(s), 1028(s), 1011(s), 997(s), 864(w), 793(m), 741(m), 690(m), 636(s), 577(w), 569(w), 507(m), 461(w).

Isolation of [U^{IV}(OSiPh₃)(dppmo)₂(OTf)₂][OTf] (2). A 20 mL scintillation vial was charged with a pale yellow solution of [U^{VI}O₂(dppmo)₂(OTf)][OTf] (125.1 mg, 0.090 mmol) in dichloromethane (2 mL). A light brown dichloromethane (2 mL) solution of Ph₃SiOTf (148.1 mg, 0.363 mmol) and Cp₂Co (31.9 mg, 0.175 mmol) was then added dropwise, which resulted in a color change to dark yellow-green. The reaction mixture was allowed to stand at room temperature for 15 h, whereupon the solution became slightly cloudy. The reaction mixture was filtered through a Celite column supported on glass wool (0.5 cm × 2 cm), concentrated *in vacuo*, and layered with diethyl ether (3 mL). Storage of this solution for 24 h at -25 °C resulted in the deposition of a yellow-green solid (123 mg). The solid was dissolved in dichloromethane (3 mL), and filtered through a Celite column supported on glass wool (0.5 cm × 2 cm). The filtrate was then concentrated *in vacuo*, and layered with diethyl ether (2 mL). Storage of this solution for 24 h at -25 °C resulted in the deposition of a crystalline mixture, which consisted of sea foam green blocks and yellow needles (total mass of 33 mg). The sea foam green blocks were characterized by X-ray crystallography, revealing the presence of [U^{IV}(OSiPh₃)(dppmo)₂(OTf)₂][OTf] (2). The presence of [Cp₂Co][OTf] was confirmed by a unit cell determination of a yellow needle: $a = 16.35 \text{ \AA}$, $b = 13.13 \text{ \AA}$, $c = 17.62 \text{ \AA}$; $\alpha = 90^\circ$, $\beta = 105.94^\circ$, $\gamma = 90^\circ$, which matches the unit cell reported for [Cp₂Co][OTf].⁴⁶ The ¹H NMR spectrum revealed the presence of both **2** and [Cp₂Co][OTf] (Figure S16) in a 2:1 ratio, respectively. ¹H NMR (CD₂Cl₂, 25 °C, 400 MHz): δ 37.86 (s, 6H, Ph₃Si ortho CH), 12.57 (s, 6H, Ph₃Si meta CH), 11.72 (s, 3H, Ph₃Si para CH), 6.36 (br s, 8H, dppmo para CH), 5.90 (br s, 16H, dppmo meta CH), 5.73 (s, [Cp₂Co]⁺), -1.80 (br s, 16H, dppmo ortho CH), -12.53 (br s, 4H, dppmo γ -CH). ¹⁹F{¹H} NMR (CD₂Cl₂, 25 °C, 376 MHz): δ -80.36 (br s, [OTf]).

[Cp₂Co][U^{IV}(OTf)₅(TPPO)₂] (3). To a cold (-25 °C) stirring yellow solution of [U^{VI}O₂(TPPO)₄][OTf]₂ (83.3 mg, 0.050 mmol) in dichloromethane (3 mL), was added cold (-25 °C) Me₃SiOTf (54 μL, 0.299 mmol) via syringe, followed by a light brown solution (-25 °C) of Cp₂Co (20.2 mg, 0.111 mmol) in dichloromethane (1 mL). This resulted in a rapid color change to yellow-green, concomitant with the deposition of a small amount of dark grey solid. The reaction mixture was allowed to stir at room temperature for 19h, whereupon it was filtered through a Celite column supported on glass wool (0.5 cm × 2 cm), which afforded a yellow-green filtrate and a small dark grey plug. The filtrate was concentrated *in vacuo*, and layered with diethyl ether (2 mL). Storage of this solution at -25 °C for 24 h resulted in the deposition of green blocks, which were isolated by decanting off the supernatant (65.6 mg, 76% yield). Anal. Calcd for UO₁₇P₂S₅F₁₅CoC₅₁H₄₀: C, 35.43; H, 2.33. Found: C, 35.38; H, 2.13. ¹H NMR (CD₂Cl₂, 25 °C, 400 MHz): δ 31.66 (br s, 12H, ortho CH), 12.04 (br s, 12H, meta CH), 11.16 (br s, 6H, para CH), 5.70 (s, 10H, [Cp₂Co]⁺). ¹⁹F{¹H} NMR (CD₂Cl₂, 25 °C, 376 MHz): δ -79.06 (br s, outer sphere [OTf]⁻), -101.02 (br s, inner sphere [OTf]⁻). UV-vis/NIR (CH₂Cl₂, 3.57 × 10⁻³ M, L·mol⁻¹·cm⁻¹): 400 (ε = 299), 634 (ε = 22), 906 (sh, ε = 7), 1054 (ε = 26), 1272 (ε = 10), 1378 (ε = 6), 1476 (ε = 7), 1994 (ε = 9). IR (KBr pellet, cm⁻¹): 1591(w), 1487(w), 1439(m), 1417(w), 1344(br m), 1319(sh m), 1259(m), 1236(s), 1203(vs), 1182(sh s), 1163(sh m), 1122(s), 1065(w), 1034(s), 1014(s), 991(vs), 865(w), 800(br w), 756(w), 750(w), 729(m), 690(m), 630(s), 584(w), 569(w), 540(s), 511(w), 507(w), 459(w).

Table 2. X-ray Crystallographic Information for 1-3

	1	2	3
empirical formula	UO ₁₉ P ₄ S ₅ F ₁₅ CoC ₈₂ H ₆₀	UCl ₆ O ₁₅ P ₄ S ₃ SiF ₉ C ₇₈ H ₆₅	UO ₁₇ P ₂ S ₅ F ₁₅ CoC ₅₁ H ₄₀
Crystal habit, color	block, yellow-green	block, sea-green	plate, yellow-green
crystal size (mm)	0.35 × 0.25 × 0.25	0.40 × 0.20 × 0.20	0.10 × 0.20 × 0.50
crystal system	triclinic	monoclinic	monoclinic
space group	<i>P</i> -1	<i>P</i> 2 ₁ / <i>n</i>	<i>P</i> 2 ₁ / <i>c</i>

vol (Å ³)	4658(2)	8559(3)	6043(1)
a (Å)	15.665(5)	17.810(3)	16.464(2)
b (Å)	15.876(5)	18.573(3)	20.580(3)
c (Å)	19.073(6)	25.953(4)	17.835(2)
α (deg)	90.641(7)	90	90
β (deg)	91.942(6)	94.423(4)	90.708(3)
γ (deg)	100.661(6)	90	90
Z	2	4	4
fw (g/mol)	2215.44	2112.18	1729.03
density (calcd) (Mg/m ³)	1.580	1.639	1.901
abs coeff (mm ⁻¹)	2.189	2.327	3.292
F ₀₀₀	2196	4200	3384
Total no. reflections	25154	90417	39529
Unique reflections	15158	17225	12364
final R indices [I > 2σ(I)]	R ₁ = 0.1029 wR ₂ = 0.2215	R ₁ = 0.0729 wR ₂ = 0.1806	R ₁ = 0.0456 wR ₂ = 0.0978
largest diff peak and hole (e ⁻ Å ⁻³)	2.483 and -3.034	3.364 and -2.335	1.489 and -0.850
GOF	0.929	1.037	1.028

Supporting Information

Experimental procedures, crystallographic details (as CIF files) and spectral data for compounds **1-3**. This material is available free of charge via the Internet at <http://pubs.acs.org>.

Acknowledgements

This work was supported by the U.S. Department of Energy, Office of Basic Energy Sciences, Chemical Sciences, Biosciences, and Geosciences Division under Contract DE-FG0209ER16067. E. A. P. thanks the NSF PIRE-ECCI program for a fellowship.

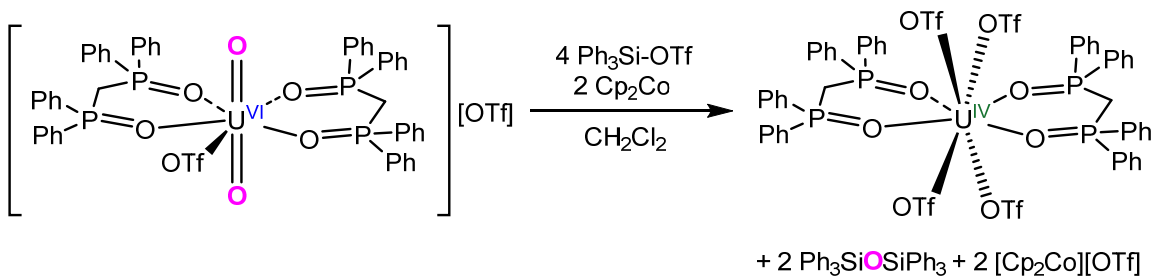
References

- (1) Arnold, P. L.; Patel, D.; Wilson, C.; Love, J. B. *Nature* **2008**, *451*, 315-318.

- (2) Arnold, P. L.; Love, J. B.; Patel, D. *Coord. Chem. Rev.* **2009**, *253*, 1973 - 1978.
- (3) Yahia, A.; Arnold, P. L.; Love, J. B.; Maron, L. *Chem. Commun.* **2009**, 2402-2404.
- (4) Yahia, A.; Arnold, P. L.; Love, J. B.; Maron, L. *Chem. Eur. J.* **2010**, *16*, 4881-4888.
- (5) Arnold, P. L.; Hollis, E.; Nichol, G. S.; Love, J. B.; Griveau, J.-C.; Caciuffo, R.; Magnani, N.; Maron, L.; Castro, L.; Yahia, A.; Odoh, S. O.; Schreckenbach, G. *J. Am. Chem. Soc.* **2013**, *135*, 3841-3854.
- (6) Jones, G. M.; Arnold, P. L.; Love, J. B. *Chem. Eur. J.* **2013**, *19*, 10287-10294.
- (7) Arnold, P. L.; Pecharman, A.-F.; Hollis, E.; Yahia, A.; Maron, L.; Parsons, S.; Love, J. B. *Nat. Chem.* **2010**, *2*, 1056-1061.
- (8) Schnaars, D. D.; Wu, G.; Hayton, T. W. *J. Am. Chem. Soc.* **2009**, *131*, 17532-17533.
- (9) Schnaars, D. D.; Wu, G.; Hayton, T. W. *Inorg. Chem.* **2011**, *50*, 4695-4697.
- (10) Schnaars, D. D.; Wu, G.; Hayton, T. W. *Inorg. Chem.* **2011**, *50*, 9642-9649.
- (11) Pedrick, E. A.; Wu, G.; Hayton, T. W. *Inorg. Chem.* **2014**, *53*, 12237-12239.
- (12) Berthet, J.-C.; Siffredi, G.; Thuéry, P.; Ephritikhine, M. *Eur. J. Inorg. Chem.* **2007**, *2007*, 4017-4020.
- (13) Brown, J. L.; Wu, G.; Hayton, T. W. *J. Am. Chem. Soc.* **2010**, *132*, 7248 - 7249.
- (14) Bagnall, K. W.; du Preez, J. G. H. *Chem. Commun.* **1973**, 820-821.
- (15) Pedrick, E.; Wu, G.; Kaltsoyannis, N.; Hayton, T. W. *Chem. Sci.* **2014**, *5*, 3204-3213.
- (16) Brown, J. L.; Mokhtarzadeh, C. C.; Lever, J. M.; Wu, G.; Hayton, T. W. *Inorg. Chem.* **2011**, *50*, 5105-5112.
- (17) Fortier, S.; Hayton, T. W. *Coord. Chem. Rev.* **2010**, *254*, 197-214.
- (18) Cornet, S. M.; May, I.; Redmond, M. P.; Selvage, A. J.; Sharrad, C. A.; Rosnel, O. *Polyhedron* **2009**, *28*, 363-369.
- (19) Casanova, D.; Alemany, P.; Bofill, J. M.; Alvarez, S. *Chem. Eur. J.* **2003**, *9*, 1281-1295.
- (20) Berthet, J.-C.; Nierlich, M.; Ephritikhine, M. *C. R. Chimie* **2002**, *5*, 81-88.
- (21) Natrajan, L.; Mazzanti, M.; Bezombes, J. P.; Pecaut, J. *Inorg. Chem.* **2005**, *44*, 6115-6121.
- (22) Maynadié, J.; Berthet, J.-C.; Thuéry, P.; Ephritikhine, M. *Organometallics* **2006**, *25*, 5603-5611.
- (23) Schnaars, D. D.; Wu, G.; Hayton, T. W. *Dalton Trans.* **2008**, 6121-6126.
- (24) Jilek, R. E.; Tomson, N. C.; Shook, R. L.; Scott, B. L.; Boncella, J. M. *Inorg. Chem.* **2014**, *53*, 9818-9826.
- (25) Charpin, P.; Lance, M.; Soulie, E.; Vigner, D.; Marquet-Ellis, H. *Acta Crystallogr. Sec. C* **1985**, *41*, 1723-1726.
- (26) Bombieri, G.; Brown, D.; Graziani, R. *J. Chem. Soc. Dalton Trans.* **1975**, 1873-1876.
- (27) Andrews, C. G.; Macdonald, C. L. B. *J. Organomet. Chem.* **2005**, *690*, 5090-5097.
- (28) Cohen, D.; Carnall, W. T. *J. Phys. Chem.* **1960**, *64*, 1933 - 1936.
- (29) Monreal, M. J.; Diaconescu, P. L. *Organometallics* **2008**, *27*, 1702-1706.

- (30) Harris, R. K.; Pritchard, T. N.; Smith, E. G. *J. Chem. Soc., Faraday Trans. 1* **1989**, *85*, 1853-1860.
- (31) Porchia, M.; Brianese, N.; Casellato, U.; Ossola, F.; Rossetto, G.; Zanella, P. *J. Chem. Soc. Dalton Trans.* **1989**, 677 - 681.
- (32) Kurfürst, M.; Blechta, V.; Schraml, J. *Mag. Reson. Chem.* **2011**, *49*, 492-501.
- (33) Pell, T. P.; Couchman, S. A.; Ibrahim, S.; Wilson, D. J. D.; Smith, B. J.; Barnard, P. J.; Dutton, J. L. *Inorg. Chem.* **2012**, *51*, 13034-13040.
- (34) Kuroboshi, M.; Yano, T.; Kamenoue, S.; Kawakubo, H.; Tanaka, H. *Tetrahedron* **2011**, *67*, 5825-5831.
- (35) Bassindale, A. R.; Stout, T. *Tetrahedron Lett.* **1985**, *26*, 3403-3406.
- (36) Wilkerson, M. P.; Burns, C. J.; Paine, R. T.; Scott, B. L. *Inorg. Chem.* **1999**, *38*, 4156-4158.
- (37) Sutton, A. D.; John, G. H.; Sarsfield, M. J.; Renshaw, J. C.; May, I.; Martin, L. R.; Selvage, A. J.; Collison, D.; Helliwell, M. *Inorg. Chem.* **2004**, *43*, 5480-5482.
- (38) Asadi, A.; Avent, A. G.; Eaborn, C.; Hill, M. S.; Hitchcock, P. B.; Meehan, M. M.; Smith, J. D. *Organometallics* **2002**, *21*, 2183-2188.
- (39) Harris, R. K.; Becker, E. D.; Cabral De Menezes, S. M.; Goodfellow, R.; Granger, P. *Pure Appl. Chem.* **2001**, *73*, 1795-1818.
- (40) Harris, R. K.; Becker, E. D.; Cabral De Menezes, S. M.; Granger, P.; Hoffman, R. E.; Zilm, K. W. *Pure Appl. Chem.* **2008**, *80*, 59-84.
- (41) SMART Apex II, Version 2.1, Bruker AXS Inc., Madison, WI, 2005,
- (42) SAINT Software User's Guide, Version 7.34a, Bruker AXS Inc., Madison, WI, 2005,
- (43) SADABS, Sheldrick, G. M., University of Gottingen, Germany, 2005,
- (44) SHELXTL PC, Version 6.12, Bruker AXS Inc., Madison, WI, 2005,
- (45) Kannan, S.; Moody, M. A.; Barnes, C. L.; Duval, P. B. *Inorg. Chem.* **2006**, *45*, 9206-9212.
- (46) Andrews, C. G.; Macdonald, C. L. B. *Acta Cryst. Sect. E.* **2005**, *61*, m2103

For Table of Contents Only



$[\text{U}^{\text{VI}}\text{O}_2(\text{dppmo})_2(\text{OTf})][\text{OTf}]$ (dppmo = $\text{Ph}_2\text{P}(\text{O})\text{CH}_2\text{P}(\text{O})\text{Ph}_2$) can be converted to $\text{U}^{\text{IV}}(\text{OTf})_4(\text{dppmo})_2$, at ambient temperature and pressure, by the synergistic action of Ph_3SiOTf and Cp_2Co .